Analytical Biochemistry 387 (2009) 30–41

Contents lists available at ScienceDirect

Analytical Biochemistry

journal homepage: www.elsevier.com/locate/yabio

FitSpace Explorer: An algorithm to evaluate multidimensional parameter space in fitting kinetic data

Kenneth A. Johnson [a,b,*], Zachary B. Simpson [b], Thomas Blom [a]

[a] KinTek Corporation, Austin, TX 78735, USA
[b] Department of Chemistry and Biochemistry, Institute for Cellular and Molecular Biology, University of Texas, 2500 Speedway, MBB 3.122, Austin, TX 78712, USA

ARTICLE INFO

Article history:
Received 10 August 2008
Available online 25 December 2008

Keywords:
Simulation
Nonlinear regression
Error analysis
Confidence intervals
Progress curve kinetics
Stopped-flow
Quench-flow
Data fitting
Enzyme kinetics

ABSTRACT

Fitting several sets of kinetic data directly to a model based on numerical integration provides the best method to extract kinetic parameters without relying on the simplifying assumptions required to achieve analytical solutions of rate equations. However, modern computer programs make it too easy to enter an overly complex model, and standard error analysis grossly underestimates errors when a system is underconstrained and fails to reveal the full degree to which multiple parameters are linked through the complex relationships common in kinetic data. Here we describe the application of confidence contour analysis obtained by measuring the dependence of the sum square error on each pair of parameters while allowing all remaining parameters to be adjusted in seeking the best fit. The confidence contours reveal complex relationships between parameters and clearly outline the space over which parameters can vary (the "FitSpace"). The utility of the method is illustrated by examples of well-constrained fits to published data on tryptophan synthase and the kinetics of oligonucleotide binding to a ribozyme. In contrast, analysis of alanine racemase clearly refutes claims that global analysis of progress curves can be used to extract the free energy profiles of enzyme-catalyzed reactions.

Common algorithms for fitting data by nonlinear regression provide a covariance matrix from which standard errors can be calculated to give an estimate of the confidence intervals on fitted parameters [1,2]. Like other data fitting programs, KinTek Global Kinetic Explorer computes standard errors based on these well-established algorithms for nonlinear regression [3]. However, these methods fail to reveal the extent to which parameters are seriously underconstrained when a model is overly complex and when the relationships between parameters and observable data are indirect, which is a common occurrence with kinetic data. In this article, we present methods to overcome the limitations of standard error analysis by more fully exploring the space over which parameters can vary in fitting the data, which we refer to as the "FitSpace," and we illustrate the method with several examples. We present a method to provide a more reliable estimate of errors on fitted parameters based on a threshold in the FitSpace contours.

Modern programs that provide fast simulation of complex models make it easy to define an overly complex model as the basis for data fitting and then to extract kinetic constants by finding a fit that conforms to the data. However, unlike conventional fitting to analytical functions, it is difficult to describe the relationships between individual fitted parameters and elements of the data that support their definition. For example, in the classical fitting of steady-state kinetic data on a double reciprocal plot, it is easy to see that the y intercept defines $1/k_{cat}$ and the slope defines $1/(k_{cat}/K_m)$, but visualizing those features that define k_{cat} and K_m in a global fit to the primary data is less obvious. Moreover, as a model gets more complex, it becomes more difficult to address the question as to whether the derived set of fitted parameters is unique and well constrained by the data. For example, in a recent nonlinear global regression analysis of full progress curves of the reaction catalyzed by alanine racemase, data were fit to extract eight rate constants [4], although we show here that the information content of the data was sufficient to define only four parameters—k_{cat} and K_m in each direction—and can place only lower limits on any intrinsic rate constant. This example illustrates how conventional error analysis fails by providing false confidence in fitted parameters that are not well constrained by the data.

Nonlinear regression represents an extension from the mathematically well-established equations for linear regression by proposing that the best fit is defined by the parameter set providing the minimum sum square error (SSE),[1] obtained by summing over all data points the square of the difference between the observed

* Corresponding author. Address: Department of Chemistry and Biochemistry, Institute for Cellular and Molecular Biology, University of Texas, 2500 Speedway, MBB 3.122, Austin, TX 78712, USA. Fax: +1 512 471 0435.
E-mail address: kajohnson@mail.utexas.edu (K.A. Johnson).

[1] *Abbreviations used:* SSE, sum square error; 3D, three-dimensional; 1D, one-dimensional; 2D, two-dimensional; 4D, four-dimensional.

0003-2697/$ - see front matter © 2008 Elsevier Inc. All rights reserved.
doi:10.1016/j.ab.2008.12.025

data and calculated value predicted by the fitted function. The function is evaluated iteratively as the parameters are adjusted until a minimum in the SSE is found with respect to each variable parameter. To evaluate complex models, the fitted function is computed by numerical integration of rate equations derived from the model rather than to the analytical solution, but the process of finding the best fit is still the same [5,6]. This enables multiple parameters to be fit simultaneously to multiple data sets based on a single kinetic model without simplifying assumptions. However, this computational power compounds the limitations inherent in nonlinear regression. Standard error values computed from the covariance matrix by nonlinear regression always underestimate the true error, in part, because the fitting process assumes that all experimental errors are uncorrelated and normally distributed, which is often not the case. In general, the distribution of errors can be approximated as normal when the number of data points is large, but experimental data often show correlated deviations from the ideal that preclude this simplification. Moreover, the covariance matrix is not valid (or does not exist) when the parameters are underconstrained by the data.

Standard error analysis results from the evaluation of errors in the dimension of each parameter at the local minimum derived for all parameters, so that the analysis fails to fully account for cases where sets of parameters are correlated and can vary systematically over a wide range of values. Although analysis of variance can reveal linear correlation coefficients between pairs of parameters, it fails to reveal more complex relationships and underestimates the full range of parameter space. The observable kinetic data, in terms of rates and amplitudes of reaction, are complex functions of multiple rate constants that are not easy to resolve. Error estimates from nonlinear regression evaluate goodness of fit for a given parameter only at the local minimum derived for the remaining parameters and do not adequately address the extent to which a given parameter is constrained independent of values assumed for other parameters. For these reasons, it is extremely difficult to evaluate whether multiple parameters are adequately constrained by the data.

Various attempts used in the past can be quite misleading. For example, simply showing that the algorithm always returns the same results regardless of starting estimates for parameters fails to provide a rigorous test and reveals more about the method used to find the local minimum than the uniqueness of the fit. Because randomly generated starting estimates covering a large range of values often lead to parameter sets that do not converge on fitting, a narrower range of values must be used and this necessarily leads to the same local minimum. Therefore, this analysis does not address the important question of whether the model is overly complex. In addition, nonlinear regression algorithms push unconstrained parameters to values that no longer affect the fitted curves. More modern approaches based on resampling, such as the bootstrap method, and Monte Carlo methods can be more reliable in some circumstances [7–9] but still suffer from producing error estimates that are overly optimistic because they fail to explore the larger space over which parameters can vary. For example, bootstrap methods failed to reject a proposed fit involving 18 parameters [10] that our methods reveal to be seriously underconstrained. One needs more than a set of algorithms that produce different tables of confidence intervals, each based on a given set of simplifying assumptions. Rather, we present a method to reveal graphically the underlying relationships between parameters and the extent to which parameters are constrained independent of assumed values for all other parameters. This analysis provides a more robust method to estimate errors on fitted parameters and clearly reveals when the parameters are underconstrained.

Our method is based on the brute force computation of confidence contours with no simplifying assumptions regarding their shape. We have developed an algorithm based on the well-documented approach to the use of constant χ^2 intervals as confidence limits on fitted parameters to explore the space over which parameters can vary [3] and to display that information graphically to afford immediate evaluation of how well the parameters are constrained by the data. This article follows from the preceding one [11] in which we described a new program for fast dynamic simulation of kinetic data. Here we use examples introduced in the accompanying article to illustrate the use of FitSpace Explorer. A free student version of the software is available at http://www.kintek-corp.com/kinetic_explorer and includes all of the examples discussed here as well as detailed instructions.

The method is based on the computation and plotting of three-dimensional (3D) confidence contours by examining the dependence of the sum square residuals (or SSE) on each pair of parameters [1]. We construct confidence contours by evaluating the dependence of SSE on pairwise combinations of parameters while allowing all other parameters to be adjusted by nonlinear regression to achieve the minimum SSE at each point on the contour. As we show here, standard error analysis fails because of the strong interdependence between the observable data and all of the fitted kinetic parameters. To fully explore the space over which all parameters are allowed to vary in achieving an adequate fit to the data, we repeat the computation of confidence contours for all pairs of parameters to construct the FitSpace. This more intensive computation defines the extent to which pairs of parameters are correlated and individual parameters are constrained by the data without assumptions regarding the magnitude of any other parameters.

The confidence contours provide a striking visual indication of overparameterized models, reveal complex relationships between parameters when they are not constrained, and provide realistic limits of error on fitted parameters. In this article, we show the results of analysis on two previously published models that are nicely constrained by the supporting experimental data and on one that is not.

Conventions

In reference to reaction schemes, steps are numbered sequentially from left to right and forward rate constants are assigned a positive step number integer, whereas the reverse rate constants are assigned a negative integer for the same step number. All second-order rate constants (involving the reaction of two species) are given in units of $\mu M^{-1}\ s^{-1}$, and all first-order rate constants are reported in units of s^{-1}.

3D confidence contours

As an approximation to evaluating the complex interrelationships among parameters in multidimensional space, we have taken the approach of constructing 3D confidence contours by pairwise evaluation of all fitted parameters, as illustrated in Fig. 1. To construct the confidence contour, we systematically vary a given pair of parameters around the area of their best fit. At each *x,y* pair of the tested parameter values, we fit the data by allowing all of the other parameters to vary in converging to the best fit while holding the *x,y* pair of parameters fixed. After convergence to the best fit, we compute the SSE. By repeating this process for all *x,y* pairs within a grid, we construct a 3D profile of the SSE as shown in Fig. 1. In this example, data from tryptophan synthase (see Fig. 1 of the accompanying article [11]) were fit to a two-step model shown in Scheme (1) (see below) involving four rate constants and two scaling factors. To compute the contour in Fig. 1, rate constants k_1 and k_{-1} were varied systematically across the *x,y* grid and the

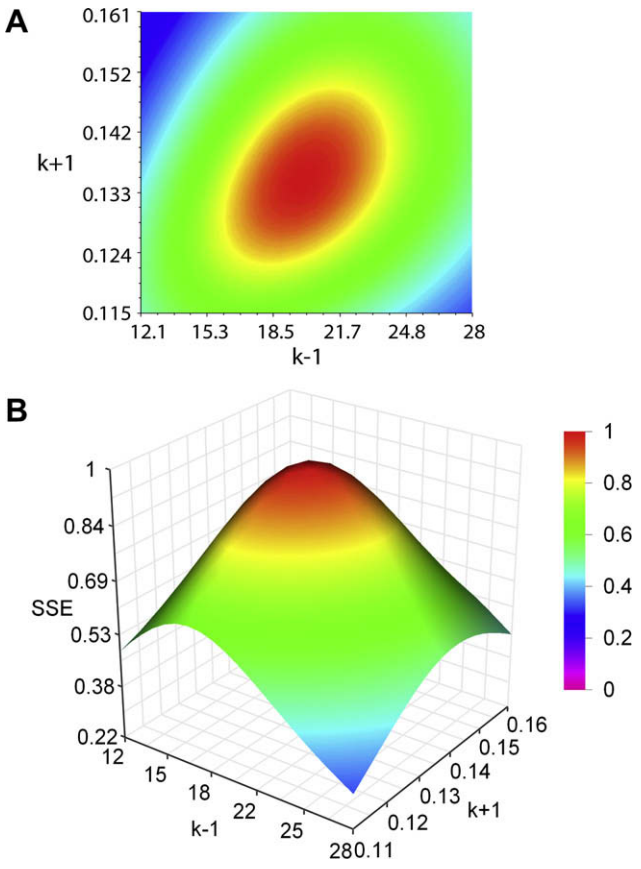

Fig. 1. Confidence contour example. (A) Two-dimensional view of contour shown in panel B. (B) Three-dimensional plot of contour derived in globally fitting tryptophan synthase data to four rate constants and two fluorescence output factors. This figure shows the dependence of the SSE on two rate constants, k_1 and k_{-1}, while varying all other parameters to achieve the best fit. The z axis displays the overall minimum SSE divided by the SSE observed at each x,y pair of k_1,k_{-1} values, $SSE_{min}/SSE_{x,y}$. The color coding provides a yellow band at the threshold of a 25% increase in SSE, where $SSE_{min}/SSE_{x,y} = 0.8$. (For interpretation of the reference to color in this figure legend, the reader is referred to the Web version of this article.)

SSE was computed after allowing the four remaining parameters to vary in achieving the best fit. Therefore, this contour evaluates the extent to which k_1 and k_{-1} are determined by the data and reveals relationships between these two parameters without any constraints imposed by the values of any other parameter. Accordingly, the confidence contour shows the extent to which each of these constants is constrained by the data.

To normalize the range of variation in SSE, and because peaks are easier to see than valleys on 3D plots, we compute the reciprocal of the normalized SSE as $SSE_{min}/SSE_{x,y}$. The z axis spans the range of 0 to 1, where 1 represents the best overall fit. Fig. 1 shows a peak in the optimal fitting, defining the best-fit values for k_1 and k_{-1}. Moreover, the 3D contour provides a measurement of the range over which the parameters k_1 and k_{-1} can vary while still achieving a good fit. Assessment of the errors in each of the parameters can be derived by analysis of the confidence contours relative to a fixed threshold in the $SSE_{min}/SSE_{x,y}$. The maximum upper and lower limits allowed for each parameter are defined by points on a fixed threshold in the SSE contour, illustrated by the yellow (or white) band on the plot (Fig. 1). The error limits attained by this approach are more realistic and reliable than the conventional error analysis based on the nonlinear regression covariance matrix, as discussed below. We are in the process of evaluating several algorithms that might reliably compute what the threshold should be based on the number of data points. The current version of the program allows the user to define a threshold, from which upper and lower boundaries on each parameter are computed by inspection of the confidence contours. This method has the advantage that more realistic error estimates are obtained especially when the confidence contours are skewed or unbounded, as illustrated by the examples below.

The following examples illustrate the use of the FitSpace confidence contours to evaluate whether a given model and set of rate constants are constrained by the data. In addition to providing more reliable estimates of errors when parameters are well constrained by the data, this analysis also reveals when a given model is overly complex by showing large areas over which parameters can vary and still achieve an acceptable fit. Eliminating overly complex models is the biggest challenge in multiparameter data fitting, and this aspect of the FitSpace Explorer calculation provides the greatest benefit.

Example 1: Tryptophan synthase

As shown in Fig. 1 of the accompanying article [11], the β-reaction catalyzed by tryptophan synthase begins by the reaction of serine with pyridoxal phosphate to form a quinonoid species (EQ) that decays by the elimination of water to form a reactive aminoacrylate ($E{\sim}A$) according to the following pathway. The formation and decay of EQ can be monitored by fluorescence, and analysis of published data by conventional fitting led to the following model [12]:

$$E + S \underset{20\ s^{-1}}{\overset{0.135\ \mu M^{-1}\ s^{-1}}{\rightleftharpoons}} EQ \underset{10\ s^{-1}}{\overset{45\ s^{-1}}{\rightleftharpoons}} E \sim A \qquad \text{(Scheme 1)}$$

$$\text{Fluorescence} = a^*[EQ] + b$$

Synthetic data were generated according to this model with added noise (normally distributed) to mimic the published results and were then fit globally based on simulation, and contours were constructed to get the results shown in Fig. 2A and Table 1A. Standard error estimates for each parameter were obtained by nonlinear regression, whereas the upper and lower limits on the fitted parameters were obtained from the 25% threshold of the confidence contour (Table 1A). In this example, nonlinear regression provides unrealistically low error estimates on the order of 1% of the value of each parameter (range of 0.5–1.9%). In contrast, error limits from the confidence contour are approximately 10% (range of 4–18%). For each parameter, the error limits from the confidence contour analysis were approximately 10-fold greater than the values obtained from nonlinear regression. In this case, where the fitted parameters are well constrained by the data and there are a large number of data points (500 per trace), standard nonlinear regression predicts very small errors in fitted parameters because these methods assume that the best fit is necessarily at the center of the distribution of errors in the data along the each segment of each trace; that is, the errors are independent and identically distributed. Accordingly, an SSE threshold of approximately 1% could be used to estimate errors in the fitted parameters. This is a valid assumption for our synthetic data. However, this is not always the case for experimental data where the data are not necessarily independently and identically distributed.

Another way to assess whether the error limits on parameters are realistic is to overlay all possible curves derived from the various combinations of fitted parameters. Fig. 3 shows the results of such graphical analysis for the tryptophan synthase data based on a 25% threshold in the confidence contours. Sets of parameters derived from the 25% boundary region of a good fit were used to generate the time courses of the reaction, and all curves were overlaid on the data and the best-fit line. In this figure, all possible sets of acceptable fitted parameters yield curves that lie within the gray

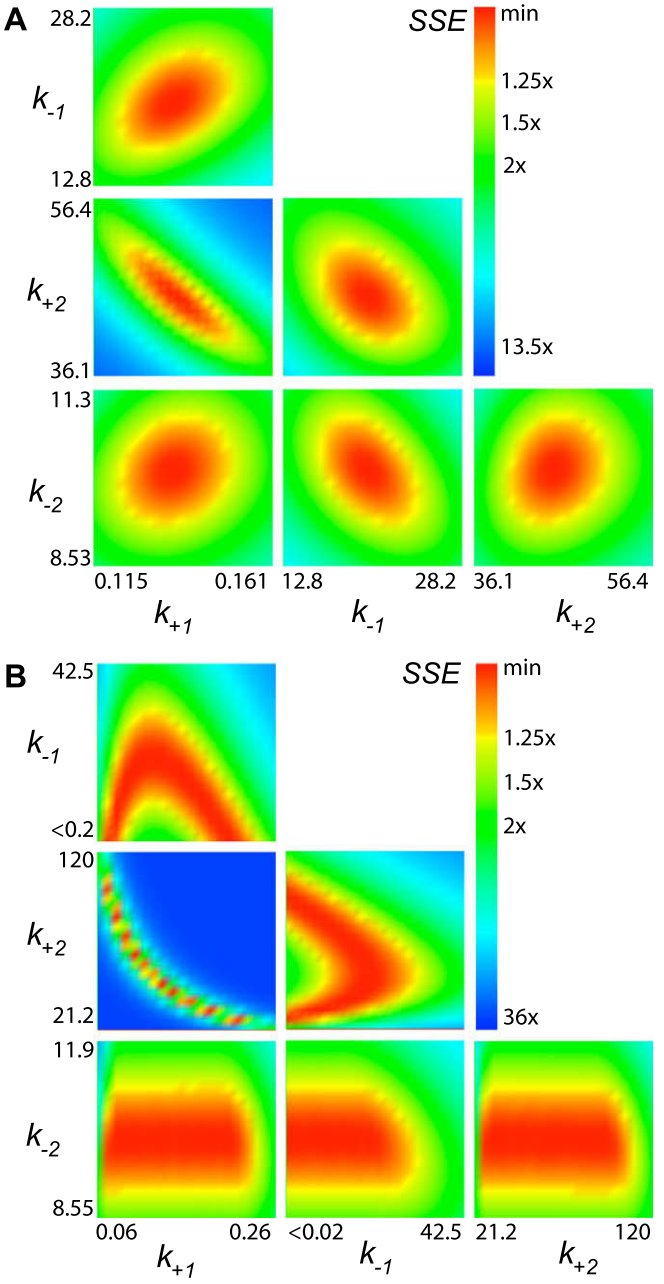

Fig. 2. Confidence contours for tryptophan synthase data fitting. (A) Confidence contours for the global fit to four rate constants and two output factors, showing all six pairwise combinations of the four rate constants. The results were derived by globally fitting the data collected at four serine concentrations (see Fig. 1 of the accompanying article [11]). (B) Confidence contours obtained by fitting four rate constants and two output factors to only one trace obtained at a concentration of 500 μM serine.

Table 1
Error analysis on tryptophan synthase parameters.

	k_{+1}	k_{-1}	k_{+2}	k_{-2}	a	b
A. Analysis of data with four traces						
Best fit	0.135	19.9	45.0	10.0	7.32	3.00
SE	0.0013	0.37	0.46	0.072	0.046	0.014
% SE	1.0	1.9	1.0	0.7	0.6	0.5
Lower	0.122	16.3	40.3	9.27	6.9	2.87
Upper	0.149	23.8	50.7	10.9	7.83	3.13
% Range	10.0	18.8	11.6	8.2	6.4	4.3
B. Analysis of data with only one trace						
Best fit	0.135	19.5	45.0	10.0	7.33	3.00
SE	0.32	28.5	118	0.35	17.6	0.048
% SE	237.0	146.2	262.2	3.5	240.1	1.6
Lower	0.066	<1e-5	24.0	9.1	4.43	2.78
Upper	0.231	29.1	108	11.1	15.7	3.19
% Range	61.1	*	93.3	10.0	76.9	6.8

Note. Artificial data were generated from the model for the tryptophan synthase reaction (Scheme 1) with added Gaussian noise to mimic the original data [12] and then were subjected to data fitting and error analysis. The best fit and standard error were derived by nonlinear regression based on numerical integration of the rate equations as described in the text. The percentage standard error (% SE) was derived from the ratio of the SE and the best fit value. Lower and upper limits were derived from the threshold of $SSE_{min}/SSE_{x,y} = 0.8$ in the confidence contours, and the percentage range (% range) was computed as (upper − lower) / (2∗best fit). The asterisk (∗) is used to indicate when there are no upper or lower limits on the parameters and percentage error would be meaningless.

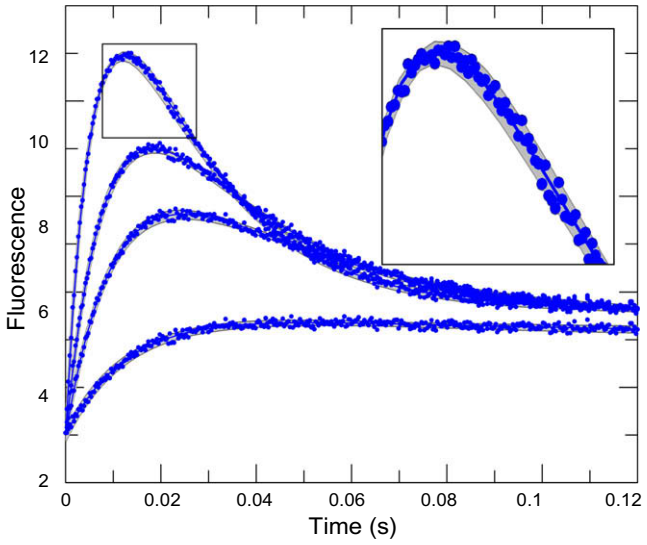

Fig. 3. Range of fitted parameters. Tryptophan synthase data were fitted globally, and sets of parameters producing a fit within 25% of the overall minimum SSE were used to generate a family of curves that were overlaid to produce the gray band. The best-fit curves are shown by the thin dark line. The inset shows a magnification of the area in the box.

boundary area. This visual representation of the data supports the conservative estimation of errors based on a 25% threshold in the SSE by showing that all possible fitted curves lay within the span of the noise in the data. More important, they lie within the span of correlated deviations typical of real data. Based on our experience in fitting real data, an SSE threshold in the range of 10 to 25% realistically evaluates allowable variations in fitted parameters based on visual examination of the fitted curves. However, as discussed in more detail below, there is no statistical basis for setting the threshold to this arbitrary value.

The most important conclusion from the analysis of the tryptophan synthase data is that the six-parameter fit is well constrained by the data. That is, the information content of the data is sufficient to define all six parameters (four rate constants and two scaling factors). As one test of our confidence contour analysis, we considered the results of fitting a single trace rather than the family of curves collected at four different serine concentrations. The results of this analysis are shown in Fig. 2B, and error analysis for this fit is shown in Table 1B. The pattern of confidence contours is clearly different, revealing that not all parameters are well constrained. In particular, it should be noted that there is no lower limit on k_{-1}. In this case, nonlinear regression returns standard error values that are larger than the value for each of the four rate constants except k_{-2}, so in this case the standard nonlinear regression algorithm provides an indication that this fit is not well defined but

does not identify the most problematic parameter. However, analysis of the confidence contours provides more informative data by placing more realistic upper and lower limits on the fitted parameters and clearly showing that k_{-1} has no lower limit within the range that was searched (down to 1e-5), but a reasonable upper limit of 29 s^{-1} was identified. Moreover, estimates of the remaining three constants can be obtained, but with 60 to 90% allowable variation in each fitted parameter.

The confidence contours reveal complex relationships between parameters. For example, the best fit over the pair of constants k_{+1},k_{+2} shows a curved dependence. Note that the discontinuous points on the figure result from our sampling on a grid, but the function is continuous and shows a curved ridge relating the best-fit parameter pairs. The relationship between k_{+1} and k_{+2} can be fit to a function where the product $k_{+1}*k_{+2}$ is a constant. This constraint can be understood as relating to the net forward rate of the two-step reaction; that is, the data constrain the product $k_{+1}*k_{+2}$ more tightly than either parameter individually.

Underlying the changes in rate constants are corresponding variations in the fluorescence output factors, which are also unknown parameters in fitting the data. By allowing the output factors to vary, a larger range of variability is seen in the rate constants. This is illustrated in Fig. 4, showing the results of every set of parameters giving a fit within 0.1% of the minimum SSE in fitting only one trace of the tryptophan synthase data. These parameter sets produce indistinguishable curves for the time course of reaction because the SSE is invariant (Fig. 4, upper panel). The value for each parameter is plotted as a function of variation in k_{+1} (note that k_2 is on a different scale on the right). This analysis shows the correlations between various parameters, similarly to the patterns shown in Fig. 2B, but includes variation in the output factors. For example, as k_{+1} is increased, both k_2 and the fluorescence scaling factor a decrease in a constant ratio to maintain the shape of the transient. Meanwhile, k_{-1} initially increases and then decreases, with a corresponding change in the net equilibrium constant. The peak in the value for k_{-1} can be understood in terms of the intricacies of fitting a double exponential function where the rate of substrate binding dominates the slow phase at low values of k_{+1} but dominates the fast phase at high values of k_{+1}. The important point, germane to this discussion, is that one trace obtained at one substrate concentration is insufficient to define all six parameters, and this is readily revealed by the contour analysis. Such uncertainty is avoided either by knowing the absolute values for the fluorescence scaling factors or by performing the experiment at multiple concentrations. Fitting the data over a series of concentrations provides sufficient information to establish the scaling factors and, therefore, to uniquely determine the rates. Alternatively, if the fluorescence scaling factors were known with certainty, then the four rate constants could be determined from the transient observed at a single substrate concentration, although with greater error estimates than afforded by the concentration series. This can be readily revealed by locking the scaling factors at a preset value and then recomputing the confidence contours (not shown).

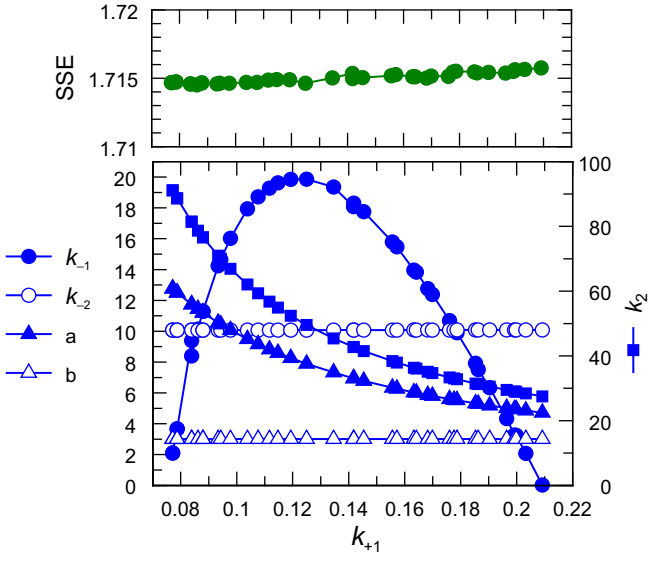

Fig. 4. Parameter variation for a poorly constrained fit. Data from the FitSpace search obtained by fitting only one trace from the tryptophan synthase data (as in Fig. 2B) were sorted to select all parameter sets that resulted in an SSE value within 0.1% of the minimum. The values of all parameters were then plotted as a function of the value of k_{+1}. The upper panel shows the SSE value obtained from each parameter set. Note that k_{-1} is plotted on a different scale (right-hand y axis).

In performing the FitSpace computation, the program first explores the space over which parameters can vary and then plots a rendition of Fig. 4 in which all parameters (including output factors) are normalized by dividing by their largest values. This puts all parameters on the same scale and allows immediate feedback regarding the extent to which parameters can vary in achieving a good fit. This is especially useful in situations where the parameters are not well constrained because it is immediately obvious from this visual display. A well-constrained fit will show all parameters clustered close to their normalized best-fit value. For example, when this parameter correlation analysis is applied to the full set of four traces for tryptophan synthase (as in Fig. 2A), all parameters cluster within 0.8 of their best-fit value.

In the current version of the software, we do not compute a full 3D contour for each output factor relative to each rate constant but rather rely on a modified rendition of Fig. 4 to reveal the underlying relationships. In a future release of the software, we will include an option to include output factors in the full FitSpace confidence contour analysis.

Example 2: Ribozyme–oligonucleotide binding

Analysis of the data obtained from the binding of a fluorescently labeled oligonucleotide to a ribozyme [13] also showed that the kinetic parameters and fluorescence scaling factors are well constrained by the data, but this example illustrates the need for an additional experiment to define the rate constants governing substrate dissociation. The family of curves resulting from the concentration dependence of the binding reaction and the competition experiment to measure the net dissociation rate (see Fig. 2 of the accompanying article [11]) were fit simultaneously to the following model:

$$E + S \underset{0.5\ s^{-1}}{\overset{3.9\ \mu M^{-1}\ s^{-1}}{\rightleftharpoons}} ES \underset{0.02\ s^{-1}}{\overset{2.5\ s^{-1}}{\rightleftharpoons}} FS \qquad \text{(Scheme 2)}$$

$$\text{Fluorescence} = a^*[ES] + b^*[FS]$$

The FitSpace confidence contour analysis for these data is shown in Fig. 5A, and errors are summarized in Table 2A. Nonlinear regression returns errors ranging from 0.03 to 2% of the parameter values. In contrast, confidence contour analysis returns error limits ranging from 0.6 to 50% and reveals that the largest errors are in the two reverse rate constants k_{-1} and k_{-2}, whereas both forward rate constants were well defined. Again, the confidence contour analysis provides a more realistic assessment of the errors in attempting to extract all four rate constants and two scaling factors from the data. It is also interesting to note that the optimal fits for the two reverse rate constants conform to a parabolic function, indicating that the data more tightly constrain the product $k_{-1}*k_{-2}$ than either parameter individually. The net observed dissociation rate measured by the second experiment (see Fig. 2B of the accompanying

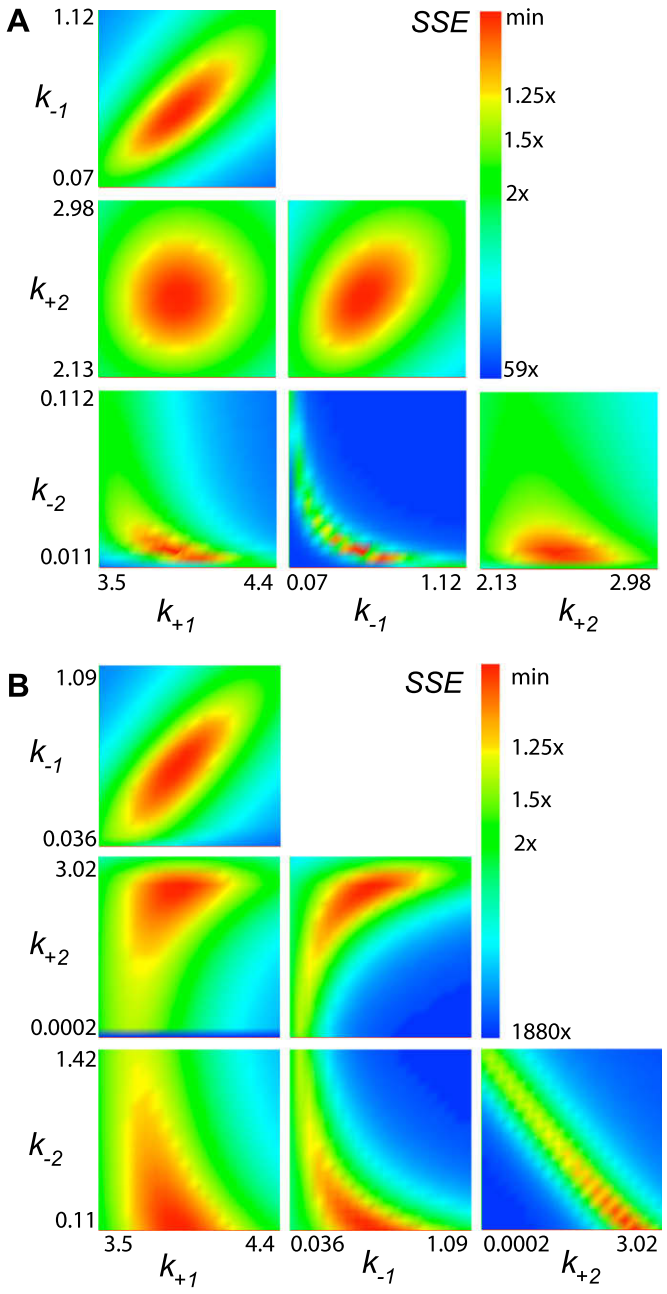

Fig. 5. Confidence contours for fitting ribozyme binding data. (A) Confidence contours were derived in globally fitting both binding and dissociation kinetic data simultaneously to the two-step model with four rate constants and one fluorescence output factor (see Figs. 2A and 2B of the accompanying article [11]). (B) Confidence contours obtained in fitting only the binding data (see Fig. 2A of the accompanying article [11]).

article [11]) can be approximated by the function $k_{obs} = k_{-1}{*}k_{-2} / (k_2 + k_{-2})$, explaining the constraint on the product $k_{-1}{*}k_{-2}$ provided by these data [13].

Even more telling are the results of the analysis of only the binding rate data (eliminating the dissociation rate data obtained in the competition experiment), as shown in Fig. 5B and summarized Table 2B. In this case, nonlinear regression returns errors on 0.3 to 235% of the fitted parameters and shows that k_{-2} is not well defined. The confidence contours reveal that k_{-2} has no lower boundary (<1e-9) but has a defined upper limit of 0.9. Errors on the other parameters range from 5 to 54%, placing more reasonable limits of error on these parameters.

Table 2
Error analysis on ribozyme parameters.

	k_{+1}	k_{-1}	k_{+2}	k_{-2}	b
A. Simultaneous analysis of data from two experiments					
Best fit	3.90	0.50	2.5	0.02	1.57
SE	0.01	0.01	0.01	0.0004	0.0005
% SE	0.3	2.0	0.4	2.0	0.03
Lower	3.7	0.28	2.31	0.014	1.56
Upper	4.12	0.79	2.76	0.033	1.58
% Range	5.4	50.2	9.0	4.6	0.6
B. Analysis of only the binding rate data					
Best fit	3.90	0.50	2.5	0.008	1.57
SE	0.01	0.01	0.01	0.019	0.0009
% SE	0.3	2.0	0.4	235	0.06
Lower	3.71	0.19	1.4	<1 e-9	1.56
Upper	4.12	0.76	2.7	0.91	1.91
% Range	5.3	54.2	25.0	*	11.1

Note. Artificial data were generated from the model for the ribozyme binding reaction with added Gaussian noise to mimic the original data [13] and then were subjected to data fitting and error analysis. Errors were computed as described in Table 1. The asterisk (*) is used to indicate when there are no lower limits on the parameters and percentage error would be meaningless.

The most important conclusion from the analysis of the ribozyme–oligonucleotide binding data is that the competition experiment is required to provide a reliable estimate of the dissociation rate constant (k_{-2}). That conclusion was already obtained by careful analysis based on conventional data fitting [13], but the current analysis is easier and more comprehensive and also provides a more realistic assessment of errors. It should be noted that the data on tryptophan synthase and the ribozyme are quite similar in that they both show biphasic fluorescence changes defining a two-step binding reaction, but there is one very important difference. In the case of tryptophan synthase, the reverse rate constants (k_{-1} and k_{-2}) were comparable to the forward isomerization rate k_{+2}; therefore, they had a significant effect on the binding kinetics and so could be resolved from analysis of the binding kinetic data alone. In contrast, the reverse rate constant k_{-2} in the ribozyme binding reaction was too small to noticeably affect the forward binding kinetics. In conventional data analysis, this distinction is revealed by fitting the data to a double exponential and then attempting to resolve the reverse rate by extrapolation of the observed rate to zero concentration (see Fig. 1B of the accompanying article [11]). In globally fitting a model directly to data, the relationships between the data and individual parameters are more difficult to see but can be clearly revealed by inspection of the confidence contours.

Example 3: Alanine racemase

Confidence contour analysis is especially critical in estimating the extent to which the fitted parameters are constrained by the data. When a model is not well constrained, nonlinear regression can be extremely misleading, as illustrated by this final example. In previously published studies, progress curves for the reaction catalyzed by alanine racemase were fit globally to define the free energy profile for the reaction based on a four-step reaction pathway, including formation and breakdown of an enzyme-bound intermediate to get the rate constants shown in Scheme (3) [4]:

$$E + L \underset{39700}{\overset{8.9}{\rightleftharpoons}} EL \underset{6.64 \times 10^8}{\overset{2650}{\rightleftharpoons}} EI \underset{4960}{\overset{2.44 \times 10^9}{\rightleftharpoons}} ED \underset{4.18}{\overset{9610}{\rightleftharpoons}} E + D. \qquad \text{(Scheme 3)}$$

However, because the data are limited to steady-state turnover as the reaction approaches equilibrium, the information content of the data is insufficient to define the rates of reaction at the active site. This can be illustrated in several ways. First, it should be noted

that the rates of breakdown of the enzyme-bound intermediate are five to six orders of magnitude faster than the rates of formation of the intermediate in each direction. Thus, the enzyme-bound intermediate is not detectable unless one has an assay sensitive enough to measure one part in a million enzyme sites. On the time scale and sensitivity of the experiment, the intermediate is not detectable. Therefore, in fitting the data globally, rate constants k_{-2} and k_3 were unconstrained by the data and assigned large values. Our attempts to compute the confidence contours with all eight parameters showed that the system is so poorly constrained that no upper limits could be found for any parameter. Moreover, dynamic simulation performed by linking k_3 and k_{-2} in a constant ratio shows that they can be reduced by five orders of magnitude before changes in the shape of the curves can be detected.

As a simple illustration of the difficulties with this model, we constructed a limited confidence contour by varying only k_{-2} and k_3 while holding all other constants fixed at their published values. Fig. 6 shows the variation in the SSE as k_{-2} was varied systematically while maintaining k_3/k_{-2} in a constant ratio ($k_3/k_{-2} = 3.67$). Deviations away from this ratio throw off the net equilibrium constant for the reaction and result in large increases in SSE, but so long as the constant ratio is maintained, the data can be fit with any pair of values approaching infinity. That is, there is no upper boundary on either parameter; however, the data do set a lower boundary on these two constants dependent on satisfying the value of k_{cat} in each direction. It should also be noted that the lower limits on k_{-2} and k_3 are dependent on the values for all other first-order rate constants in the pathway. In the limit where k_2 and k_4 are large, $k_3 = k_{cat}$ in the forward direction, whereas in the limit where k_{-3} and k_{-1} are large, $k_{-2} = k_{cat}$ in the reverse direction. Another possible fit is illustrated in the second plot in Fig. 6 (dashed line), where k_{-2} and k_3 are varied in the same constant ratio but with a different set of the remaining parameters. Here a local minimum is observed because of the choice of the remaining parameters (see figure legend). Simply stated, there are too many parameters to achieve a meaningful fit other than to extract values for k_{cat} and k_{cat}/K_m in each direction. The model is too complex. Nonetheless, nonlinear regression returns relatively small error estimates on each of the eight parameters (2.6–8% reported [4]) even though none of the parameters is well constrained by the data. This is explored in more depth by working to fit the data to a simpler model.

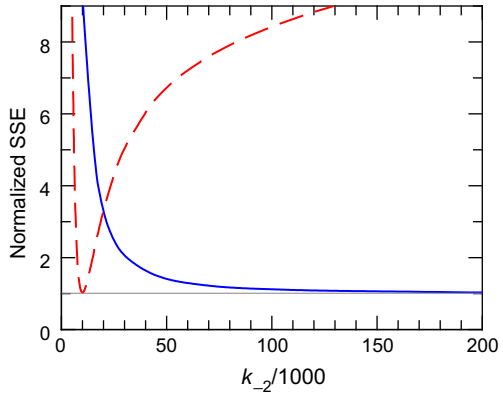

Fig. 6. Error analysis in varying only two rate constants for alanine racemase data. The alanine racemase data were modeled according to the published model with a four-step mechanism with eight rate constants. Six rate constants were held fixed at their published values, whereas k_{-2} and k_3 were varied while maintaining a constant ratio of $k_3/k_{-2} = 3.67$, and at each value the SSE was calculated (solid blue line). The *y* axis shows the SSE normalized by dividing by the minimum value. Values of k_{-2} are given in units of $s^{-1}/1000$. The process was repeated for another set of parameters revealing another local minimum in SSE obtained when $k_1 = 7.41\ \mu M^{-1}\ s^{-1}$, $k_{-1} = 36{,}000\ s^{-1}$, $k_2 = 2980\ s^{-1}$, k_{-2} and k_3 varied in constant ratio, $k_{-3} = 5760\ s^{-1}$, $k_4 = 9230\ s^{-1}$, and $k_{-4} = 3.62\ \mu M^{-1}\ s^{-1}$ (red dashed line). This figure shows only two of an infinite number of sets of parameters that afford the same minimum SSE. (For interpretation of the references to color in this figure legend, the reader is referred to the Web version of this article.)

As one example, synthetic data generated from the published model and rate constants (Scheme 3) could be fit to the following simplified model:

$$E + L \underset{388000}{\overset{(100)}{\rightleftharpoons}} EL \underset{990}{\overset{1580}{\rightleftharpoons}} ED \underset{(100)}{\overset{245000}{\rightleftharpoons}} E + D. \qquad \text{(Scheme 4)}$$

In this model, by assuming diffusion-limited substrate binding ($100\ \mu M^{-1}\ s^{-1}$), we are essentially fitting the data set only to derive k_{cat} and K_m in each direction, for example, $k_{cat} = k_2 = 1580\ s^{-1}$ and $K_{m,L} = 3880\ \mu M$ in the forward direction. The confidence contours for this fit are given in Fig. 7A, showing that each parameter is well constrained because we are fitting only four parameters to extract four meaningful kinetic constants. The information content of these steady-state data is limited to deriving only steady-state kinetic parameters. The concentration dependence of the rate defines k_{cat}/K_m, and the extrapolated maximum rate defines k_{cat} in each direction to provide four known parameters sufficient to constrain four constants but not six. One might consider that the net equilibrium constant provides a fifth known parameter, but that information is redundant once k_{cat}/K_m in each direction is established because the net equilibrium constant is equal to the ratio of k_{cat}/K_m in the forward direction divided by that in the reverse direction.

As another example, the data can also be fit to the following rate constants, giving the same values for k_{cat} and k_{cat}/K_m as derived from the more complex four-step model:

$$E + L \underset{6650}{\overset{1.46}{\rightleftharpoons}} EL \underset{1790}{\overset{3590}{\rightleftharpoons}} ED \underset{1.83}{\overset{4190}{\rightleftharpoons}} E + D. \qquad \text{(Scheme 5)}$$

To assess the extent to which all six rate constants are constrained by the data, we constructed a confidence contour for fitting data to the complete three-step model:

$$E + L \underset{k_{-1}}{\overset{k_1}{\rightleftharpoons}} EL \underset{k_{-2}}{\overset{k_2}{\rightleftharpoons}} ED \underset{k_{-3}}{\overset{k_3}{\rightleftharpoons}} E + D. \qquad \text{(Scheme 6)}$$

Synthetic data were generated from the published rate constants for the four-step model (Scheme 3) and then subjected to data fitting to the three-step model to generate the confidence contours shown in Fig. 7B. For each parameter, the contour analysis indicates a lower limit for each parameter, which is difficult to see on each graph at this magnification, but no upper limit, as summarized in Table 3B. Interestingly, the lower limits set on k_2 and k_3 are approximately equal to $k_{cat} = 1570\ s^{-1}$ in the forward direction. Correspondingly, the lower limits set on k_{-1} and k_{-2} are approximately equal to $k_{cat} = 980\ s^{-1}$ in the reverse direction. The lower limits for the second-order rate constants for substrate binding (k_1 and k_{-3}) are slightly larger than $k_{cat}/K_m = 0.4\ \mu M^{-1}\ s^{-1}$ in each direction. This is because the rates of substrate release must be comparable to the forward net reaction rate, and therefore, kinetic partitioning to release bound substrate is significant. Note that k_{cat}/K_m is defined by the second-order rate constant for substrate binding times the probability that the bound substrate continues forward to be released as product. Thus, the global fitting sets a lower limit on k_1 that is greater than k_{cat}/K_m by a factor equal to the minimal kinetic partitioning of bound substrate sufficient to account for its release in the reverse rate.

The confidence contour analysis also reveals two other interesting limits on the magnitude of individual kinetic parameters, as shown in Fig. 8. The pattern of all possible values relating k_{-1} and k_{+1} is complex. First, the contour establishes lower limits for each parameter at $k_{-1} \geqslant 980\ s^{-1}$ and $k_{+1} \geqslant 0.64\ \mu M^{-1}\ s^{-1}$ (Table 3B). Beyond those limits, any values for k_{-1} and k_{+1} are allowed so long as the ratio of k_{-1}/k_{+1} is greater than the $K_{m,L}$ for the

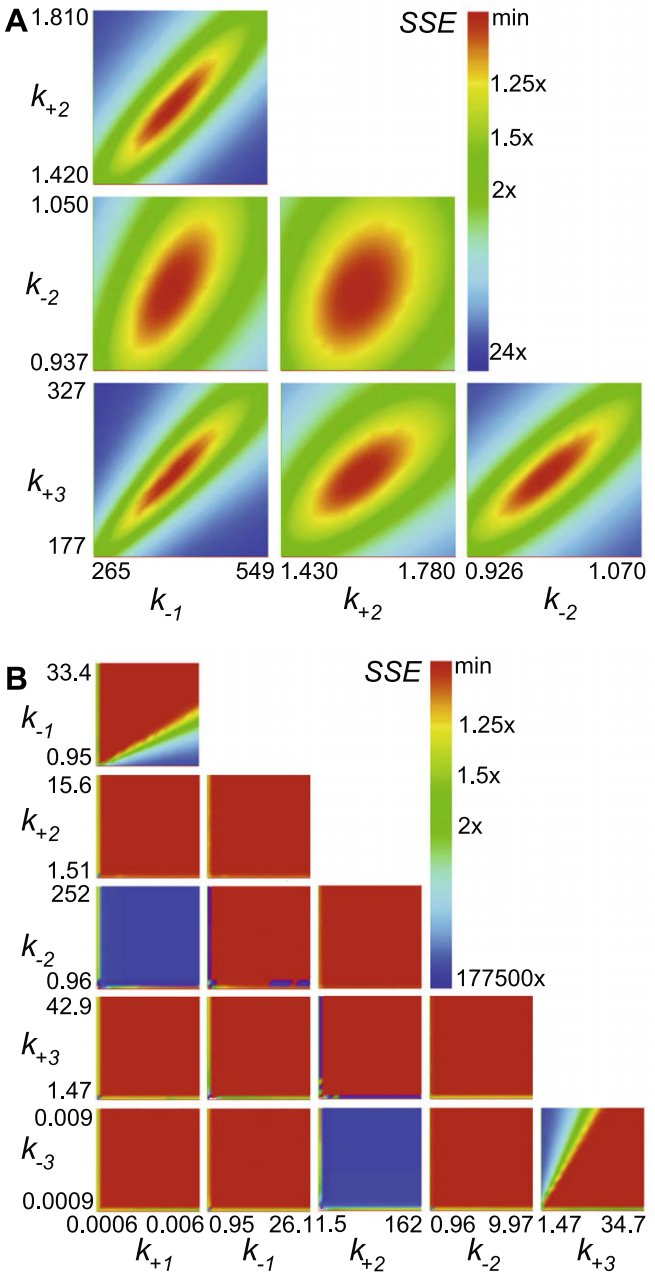

Fig. 7. Confidence contour in fitting alanine racemase data to a three-step model. (A) The alanine racemase data, generated from the four-step model with published rate constants, was fit to a three-step model with only four constants varied during the fitting process to derive this confidence contour. The rate constants for binding, $k_{+1} = 100\ \mu M^{-1}\ s^{-1}$ and $k_{-3} = 100\ \mu M^{-1}\ s^{-1}$, were held fixed while the remaining constants governing chemistry and product release in each direction were allowed to vary. The shape of these contours depends on the arbitrary choices for k_{+1} and k_{-3}. (B) These confidence contours were derived by fitting the alanine racemase data to a three-step model while varying all six rate constants. Note that in both panels, the rates are given in thousands; that is, k_{-1} ranges from 1420 to 1810 s^{-1} in panel A, whereas it ranges from 950 to more than 33,400 s^{-1} in panel B.

substrate, as defined by the sharp diagonal boundary. Thus, the data place a lower limit on the K_d for substrate binding at $K_{d,L} \geqslant K_{m,L}$. Including a reversible internal equilibrium into the model allows that K_d can be greater than K_m. In the current case, the requirement to fit both forward and reverse reactions sets only a lower limit on the K_d for substrate binding that must be greater than K_m. The same is true for the reverse reaction, as revealed by the confidence contour relating k_{-3} and k_3 and showing that $k_3/k_{-3} \geqslant K_{m,D}$.

Table 3
Error analysis on racemase parameters.

	k_{+1}	k_{-1}	k_{+2}	k_{-2}	k_{+3}	k_{-3}
A. Fitting data to only four constants						
Best fit	(100)	387900	1582	990	245608	(100)
SE	–	2870	4.6	1.7	1550	–
% SE	–	0.7	0.3	0.2	0.6	–
Lower	–	323000	1490	949	208000	–
Upper	–	464000	1790	1030	288000	–
% Range	–	18	9	4	16	–
B. Fitting data to six constants						
Best fit	1.32	5200	3206	1969	4977	2.02
SE	0.017	120	57	26	118	0.035
% SE	1.3	2.3	1.8	1.3	2.4	1.7
Lower	0.642	982	1480	1010	1580	1.02
Upper	> 21.4	>7e5	>3e7	>8e6	>1e6	>368
% Range	*	*	*	*	*	*

Note. Artificial data were generated from the model for the alanine reaction (Scheme 3) with added noise to mimic the original data [4] and then were subjected to data fitting and error analysis. Errors were computed as described in Table 1. The asterisk (*) is used to indicate when there are no upper limits on the parameters and percentage error would be meaningless.

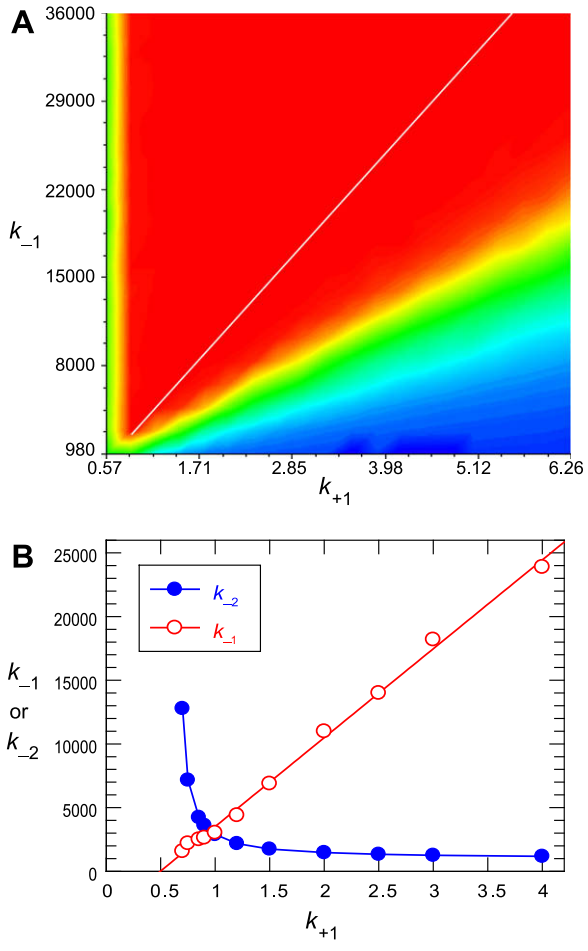

Fig. 8. Complex relationships in confidence contours. (A) A close-up view of the confidence contour of k_{-1} versus k_{+1} from Fig. 7B. The white line is the curve showing the fit given by the open circles in panel B. (B) Analysis of the relationships among k_{-1}, k_{-2}, and k_{+1}. The alanine racemase data were fit to the three-step model with all six rate constants but while systematically varying k_{+1}. Each set of points on this curve represents a fit that was achieved yielding an SSE within 1% of the minimum and indistinguishable from the best overall fit. Only the dependences of k_{-1} and k_{-2} on the fixed value of k_{+1} are shown. Other rate constants did not show a uniform trend. Units on the *y* axis are s^{-1}, whereas k_{+1} is shown in units of $\mu M^{-1}\ s^{-1}$.

Another pair of complex relationships is revealed between k_{+1} and k_{-2} and between k_{-3} and k_2. The confidence contour of k_{-2} versus k_{+1} shows only a narrow range of acceptable combinations of these two parameters. As the lower limit of k_1 is approached, the values of k_{-2} can be quite large, but as k_1 increases, k_{-2} approaches its limit set by k_{cat} in the reverse direction. This relationship is not immediately obvious because it results from fitting the forward and reverse data simultaneously. Above the minimal threshold, as k_1 increases, k_{-1} increases in a constant ratio defined by K_1. However, once k_{-1} is greater than k_{cat} in the reverse direction, k_{-2} determines the value for $k_{cat,rev}$. A similar analysis applies to understanding the relationship between k_{-3} and k_2, where as k_{-3} and k_3 increase in constant proportion, k_2 approaches the limit set by $k_{cat,for}$. Of course, this careful analysis of the confidence contours is useful only in setting limits on parameters, which in this case are not well constrained by the data.

This analysis is presented only to show that the confidence contours can be understood even when the relationships are complex. In running the computer program, an initial exploration of the space over which parameters can vary reveals the extent to which parameters are ill constrained, so that the time-consuming full FitSpace contour calculation can be stopped. Moreover, the lower limits set on parameters are reasonable based on an understanding of the reaction kinetics and the data.

Our analysis shows that the synthetic idealized data do not support reliable estimates for the eight rate constants of the four-step model as claimed in the original publications. Michael Toney kindly provided his original data, which included experiments at several enzyme concentrations as well as various substrate concentrations. Analysis of the original data yielded identical conclusions; one cannot extract free energy profiles from global fitting of progress curve kinetics. Progress curves are essentially steady-state data allowing the reaction to run to completion, and as such they afford definition of only two parameters in each direction of the reaction: k_{cat} and K_m. Our analysis shows unequivocally that one cannot derive estimates of eight parameters by global analysis of full progress curves of enzyme-catalyzed reactions, and the free energy profiles cannot be obtained from these data [4]. This error was compounded in a subsequent study in which 18 parameters were fit to data collected using deuterated substrates in attempts to extract hydrogen kinetic isotope effects [10]. This extreme overparameterization of data does not hold up to scrutiny; rather, only the effects of the deuterium substitution on k_{cat} and k_{cat}/K_m can be defined from these data. It is hoped that our new algorithm will help to prevent such errors in the future.

When and why standard methods of error analysis fail

Methods commonly employed to estimate errors on fitted parameters examine the dependence of the SSE in only one dimension, that of the parameter in question. However, the extent to which a given parameter is allowed to vary is constrained by the values chosen for other fitted parameters; therefore, the real error in the fitted parameter is greatly underestimated. This is illustrated in Fig. 9, using the fitting of the alanine racemase data as an example with the rate constants shown in Schemes (7) and (8). We begin with the case where the formation of the intermediate is rate-limiting according to the rate constants suggested previously [4] but with k_3 and k_{-2} reduced somewhat in attempts to observe greater effects of these parameters on the fit:

$$E + L \underset{39700}{\overset{8.9}{\rightleftharpoons}} EL \underset{1.1\times10^5}{\overset{2650}{\rightleftharpoons}} EI \underset{4960}{\overset{4.05\times10^5}{\rightleftharpoons}} ED \underset{4.18}{\overset{9610}{\rightleftharpoons}} E + D. \qquad \text{(Scheme 7)}$$

The one-dimensional search for the best fit for the parameter k_{-2} is shown in Fig. 9A, indicating a tight distribution that suggests very little error on the rate. A similar effect is seen in a one-dimensional (1D) search involving k_3 (not shown) and with rate constants three to four orders of magnitude lower than published [4]. This 1D search forms the basis for the low standard error estimates on each

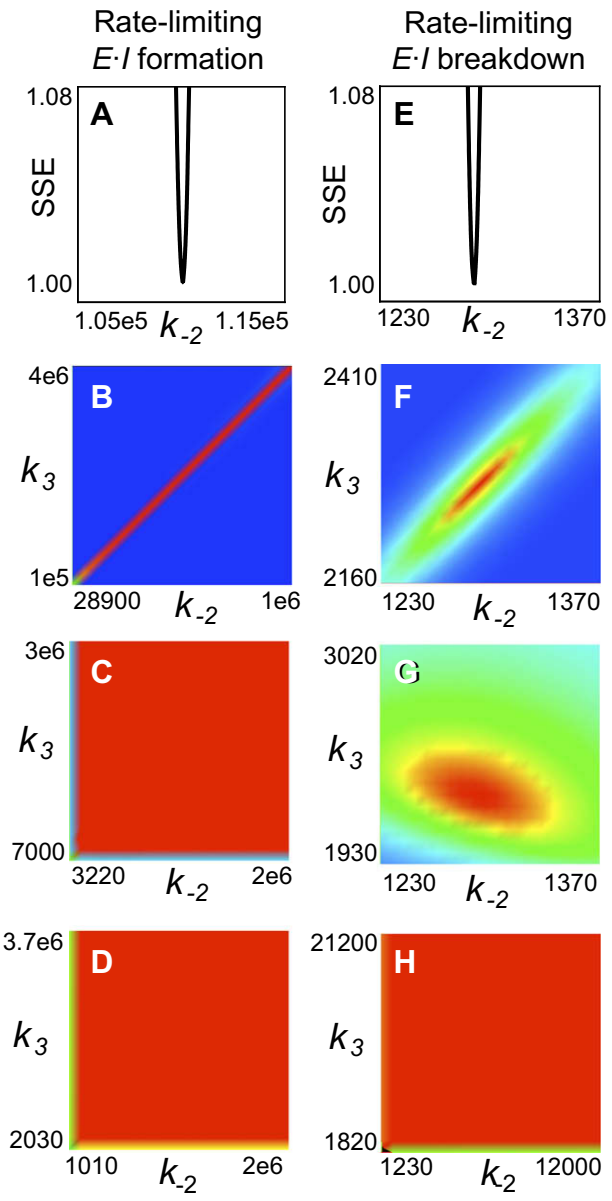

Fig. 9. Effect of parameter search dimension on observed contour. Here the confidence contours are computed with differing numbers of variable parameters for two cases. In panels A to D, the formation of the *E•I* intermediate is rate-limiting (Scheme 7), whereas in panels E to H, the breakdown of the *E•I* intermediate is rate-limiting (Scheme 8). In the first row (A,E), only k_{-2} is varied in seeking the minimum SSE. The second row (B,F) shows a standard two-parameter search in which both k_{-2} and k_3 are varied. The third row (C,G) shows a four-parameter search in which k_3 and k_{-2} are varied systematically while k_2 and k_{-3} are also allowed to be adjusted in seeking the minimum SSE. The fourth row (D,H) shows a six-parameter search in which k_3 and k_{-2} are varied systematically while k_2, k_{-3}, k_{-1}, and k_4 are also allowed to be adjusted in seeking the minimum SSE. In each three-dimensional plot, the contours are colored as in Fig. 7 and the boundary at 20 to 25% increase in SSE is given by the yellow band surrounding the red center. In the gray scale rendition, the center is dark surrounded by a light band. Panels C, D, and H are all red with the exception of a thin band defining a lower limit. The numbers on the axes define the lower and upper extents of each graph. All rate constants are in units of s^{-1}. Note that the range for the *x* axis is identical in panels E to H but vary widely in panels A to D. (For interpretation of the references to color in this figure legend, the reader is referred to the Web version of this article.)

individual parameter (Table 3). However, a two-dimensional (2D) search (Fig. 9B) reveals the linear covariation between k_3 and k_{-2} and shows that any value above a lower threshold provides a good fit so long as the ratio of k_3/k_{-2} is constant. Analysis of the covariance matrix can reveal that k_3 and k_{-2} are correlated and warn the user of a possible problem, but the true magnitude of the problem is underestimated. Moreover, as the fitting program recognizes the covariation, the values of k_3 and k_{-2} tend to increase in a constant ratio during successive rounds of fitting until further increases no longer lead to reductions in SSE. Thus, the rate constants are pushed to a high value with no constraints, but the reported errors are small based on the 1D error analysis. This explains why the regression analysis returned such large values for k_3 and k_{-2} [4]. However, even the ratio of k_3/k_{-2} is not known with certainty, and Fig. 9B is misleading because the allowed values for k_3 and k_{-2} are constrained by the values chosen for other rate constants in the pathway. This is revealed by the four-dimensional (4D) parameter search shown in Fig. 9C, where k_3 and k_{-2} are varied systematically but k_2 and k_{-3} are also allowed to be adjusted in seeking the minimum SSE (all other rate constants are held fixed). In this case, one can see that above a lower limit there are no restrictions on the individual values of k_3 and k_{-2}. They are simply not constrained by the data. A six-parameter search continues this trend (Fig. 9D).

A different pattern, but with the same conclusion, is obtained if one considers the case where the breakdown of the intermediate is rate-limiting according to Scheme (8) and illustrated in Figs. 9E–H:

$$E + L \underset{88600}{\overset{3.06}{\rightleftharpoons}} EL \underset{1290}{\overset{23200}{\rightleftharpoons}} EI \underset{118000}{\overset{2270}{\rightleftharpoons}} ED \underset{5.11}{\overset{435000}{\rightleftharpoons}} E + D. \qquad \text{(Scheme 8)}$$

Again, a 1D search of parameter k_{-2} (Fig. 9E) or k_3 (not shown) suggests a well-constrained parameter with a steep change in SSE as the parameter is changed from its best-fit value, and nonlinear regression returns an unrealistically low standard error. A 2D parameter search (Fig. 9F) reveals covariation between k_3 and k_{-2}, but unlike in Fig. 9B, both parameters show an upper boundary and a lower boundary. These boundaries exist only because of constraints imposed by values assumed for other parameters. Fig. 9G shows the results of the four-parameter contour analysis in which k_3 and k_{-2} are varied systematically, while k_2 and k_{-3} are also allowed to be adjusted in seeking the minimum SSE. Note that in this case the range allowed for variation in k_3 and k_{-2} is larger, but it is still constrained by the limitations imposed by other rate constants in the pathway that are held fixed. When constraints imposed on k_{-1} and k_4 are lifted, the full range of allowed variation in k_3 and k_{-2} is revealed in the six-parameter search (Fig. 9H).

What is clear from this analysis is that Spies and coworkers [4,10] assumed that the formation of the enzyme-bound intermediate was rate-limiting, and this assumption placed their choice of rate constants into a different domain than if they had assumed that the breakdown of the intermediate was rate-limiting in net product formation. However, many solutions exist in fitting their data. Their steady-state data provide insufficient information to define the rates of formation and decay of the intermediate at the active site. Thus, using "random" variation of starting estimates for nonlinear regression failed because the range of sampling was too small and the systematic relationships among parameters were underappreciated. Standard statistical analysis involving *F* tests or bootstrap methods also failed for similar reasons [10] because they are based on examination of the SSE in the dimension of each parameter while holding other parameters fixed at the values giving a local minimum. The standard search algorithms simply fail to look over a sufficiently wide range of parameter space to reveal the complex interdependence of kinetic parameters and observable data. Moreover, when the system is underconstrained, the covariance matrix cannot be reliably calculated because of division by terms close to zero.

In most instances, essentially every observable feature of kinetic data is a function of nearly all kinetic parameters. Consider again the data obtained using tryptophan synthase (Fig. 1 of [11]). The time dependence of the reaction can be fit to a double exponential function, providing two amplitudes, two rates, a starting value, and an endpoint of the fluorescence at each concentration. The substrate concentration dependence of the rates and amplitudes was sufficient to constrain a six-parameter fit. However, it must be noted that all observable features of the data (rates and amplitudes of reaction) are a function of all four rate constants. Analytical solution of the rate equations reveals that the two rates are defined by the roots of the quadratic equation,

$$\lambda_{1,2} = \frac{(k_1[S] + k_{-1} + k_2 + k_{-2}) \pm \sqrt{(k_1[S] + k_{-1} + k_2 + k_{-2})^2 - 4 \cdot (k_1[S] \cdot (k_2 + k_{-2}) + k_{-1}k_2)}}{2},$$

and the amplitudes are a function of the relative rates plus the scaling factors. Thus, in fitting kinetic data, no single rate constant can be obtained without allowance for the effects of all other rate constants on the magnitude of the observed rate. However, these relationships are revealed by the shape of the SSE confidence contour. The FitSpace algorithm resolves the interdependence of kinetic parameters by searching for the extremes allowed for each parameter individually while considering all possible combinations for all other parameters. The user can control the range over which the parameter search is conducted surrounding a local minimum by setting thresholds in SSE and setting limits on the magnitude of each parameter variation. Moreover, dynamic simulation allows a rapid manual search through parameter space to search for alternate local minima.

Setting the threshold for error analysis

Estimation of the errors on fitted parameters is a complex problem. Linear or nonlinear regression analysis underestimates errors because it assumes that all data are independently and identically distributed and it fails to account for all sources of error such as those arising from variable concentrations of reagents in the experiment. More important, standard analysis of variance fails to account for complex relationships between sets of fitted parameters. Thus, when reporting standard error based on regression analysis, one must always qualify the results by noting that the reported error is a minimum estimate. In spite of being generally recognized as an underestimate, the reporting of standard error on fitted parameters has become a required and accepted component in publishing scientific data. The results presented here show that even when parameters are well constrained by the data, such as in the case of the tryptophan synthase data, algorithms commonly employed to compute standard error underestimate the allowable range on the six parameters that produce acceptable fits. By examining the dependence of the SSE on parameters individually, a very steep dependence of SSE on each parameter leads

to a small standard error. However, by allowing all of the remaining parameters to float while inspecting the range over which a given pair of parameters can vary in achieving an optimal fit, the confidence contour analysis provides a more realistic assessment of the constraints on each parameter. This effect is seen in each of the examples shown but most dramatically reveals when the fitted parameters are underconstrained.

We propose that setting parameter errors based on a threshold in the SSE provides the most realistic estimate of the range over which parameters can vary while still achieving an acceptable fit. It is well accepted that confidence limits on parameters can be derived from a threshold in the SSE. For example a common expression for setting the threshold is based on the *F* distribution [1,2]:

$$\frac{\mathrm{SSE}_{\mathrm{limits}}}{\mathrm{SSE}_{\mathrm{min}}} = 1 + \frac{p}{n-p} F^{\alpha}_{p,n-p}, \tag{1}$$

where p is the number of parameters, n is the number of points, and α defines the $(1 - \alpha)*100\%$ confidence interval and the F distribution, $F^{\alpha}_{p,n-p}$, is computed for p and $n - p$ degrees of freedom. Although Eq. (1) justifies the use of a fixed threshold in the confidence contours, the value of the computed threshold underestimates errors on fitted parameters because it does not fully account for situations where data are not independently and identically distributed or where the parameters are seriously underconstrained. When the system is underconstrained, higher order terms in the SSE expansion are neglected, but they dominate the shape of the confidence contours. When the system is well constrained, Eq. (1) underestimates errors in parameter fits to real data because it assumes that there are no deviations from ideal behavior such as those due to fluctuations in lamp intensity or minor flow artifacts in a stopped-flow experiment.

Our method to conduct the confidence contour search accounts for variations due to statistical sampling by setting a fixed threshold in the SSE for each experiment. However, we have not yet found an appropriate function to predict the threshold. In this article, we have illustrated the method with a threshold set at a 25% increase in SSE, which provides a conservative estimate of the confidence in each parameter, although a 10% increase in SSE may represent a more realistic threshold to establish errors in the cases described. Although there is no statistical basis for a fixed arbitrary threshold, we have found a 10 to 25% increase in SSE to be a useful standard derived from our experience in fitting dozens of data sets with a wide range of mechanisms, with varying numbers of fitted parameters, and with various numbers of data points and differing signal/noise ratios. In the program, the user can set the threshold while the graphical display and a table showing upper and lower limits on parameters are updated. The set threshold is seen as the yellow band in the $\mathrm{SSE}_{\mathrm{min}}/\mathrm{SSE}_{x,y}$ function in the colored version of the confidence contours (available online) or as the light band surrounding the dark center in the black-and-white (print) rendition. We suggest that users report the following statistical information to describe the errors in fitting: number of data points, average sigma value (obtained from the nonlinear regression), threshold used for the SSE contours, and range of values allowable for each parameter based on that threshold.

It should be noted that the use of the fixed threshold correctly identified the lower limit for each forward rate constant in the alanine racemase four-step model as equal to k_{cat} in that direction (k_2, $k_3 \geqslant k_{\mathrm{cat}}$), and the same is true for the reverse rate constants. The differences due to the value chosen for the threshold are relatively minor in terms of the estimates of errors reported here. For example, the lower limits on k_3 for the racemase reaction are given as 1580, 1580, and 1560 s^{-1} for SSE thresholds of 1, 10, and 25%, respectively. In contrast, standard statistical analysis using *F* tests and bootstrap methods failed in that they supported the erroneous conclusion that k_3 was six orders of magnitude larger and known within 10% error and failed to reject a proposed fit involving 18 parameters [10]. Thus, the very real danger of existing statistical tests as applied to fitting multiple kinetic parameters is that they can give false confidence in the certainty of fitted parameters that are not well constrained.

Summary

Computer simulation now makes it easy to enter complex models to fit data, but the relationships between individual parameters and the experimental data are obscured by the process of simultaneously fitting multiple parameters to multiple data sets. Too often, overly complex models are proposed and parameters are extracted without a means to assess whether the data can support the model. Therefore, it is especially important to establish guidelines for use in fitting and a method to reveal the extent to which parameters are constrained by the data. The FitSpace confidence contour analysis described here fulfills that need. Thus, as was done in the case of alanine racemase, the simulation program can be used to replicate published data, which can then be evaluated to establish whether even idealized data with a normal distribution of noise can support the model. Moreover, the dynamic simulation with visual evaluation of the predicted curves allows large jumps in parameter space to evaluate whether different sets of parameters or combinations of linked constants can account for the data equally well. This use of the program was critical in jumping from the region of parameter space where the formation of the alanine racemase intermediate was rate-limiting to the region where the breakdown of the intermediate was rate-limiting (Fig. 9). This large jump requires adjustment of multiple parameters, a process that is facilitated by the use of visual feedback with dynamic simulation.

The examples shown here were chosen to illustrate the utility of the FitSpace confidence contour analysis both in providing realistic error estimates on fitted parameters when the model is well constrained by the data and in giving a dramatic visual clue when parameters are not well constrained. Several computer programs are available for fitting multiple data sets simultaneously to a single model (discussed in Ref. [11]), but all rely on error estimates from nonlinear regression and fail to reveal when parameters are not well constrained by the data. The combination of dynamic simulation with graphical analysis described in the accompanying article [11] with the confidence contour analysis presented here overcomes the limitations of standard nonlinear regression when applied to multiparameter fitting. In particular, the example of alanine racemase shows the pitfalls of the standard analysis, where nonlinear regression and bootstrap methods greatly underestimated the errors on the parameters, misleading the user into believing parameters were well constrained when they were not. The basis for this underestimate lies at the heart of the method where the effect of variation in each parameter on the net SSE is examined in the dimension of that parameter and then covariation between parameters is examined. In the case of alanine racemase, nonlinear regression underestimates the full extent of the strong correlations between parameters in the overly complex four-state model.

Computation of confidence contours is often dismissed as not generally feasible because of their expense computationally [1]. However, the brute force computation of confidence contours is feasible with modern computers and optimized code. Computations of confidence contours described here with well-constrained parameters were completed in 2 to 3 min (Figs. 2 and 5), whereas the less constrained model (Fig. 7B) required approximately 17 min to complete, each using a 2.5-GHz Intel xeon processor.

This minor investment in computation time is trivial relative to the distinct advantages offered by this analysis.

The confidence contour analysis produces visually rich feedback to show the extent to which parameters are constrained by the data and to reveal complex relationships between sets of parameters. Moreover, by allowing modest deviations from the ideal fit in exploring the parameter space, the effects of non-Gaussian errors in the data can also be evaluated. Relative to the very large errors in logic based on underestimation of errors by the standard methods, error analysis based on a threshold in the confidence contours is much more robust. For now, the 10% threshold in the SSE contours allows comparison of the results of various data sets when fit to multiple parameters and provides an important and clear indication when parameters are not well constrained by the data. The threshold can be set in the KinTek Global Kinetic Explorer program so that it can be modified as additional experience is accumulated and as we explore possible functions for predicting the threshold. Eliminating overly complex models from consideration, highlighting the need for additional experimental evidence, and cautioning against overinterpretation, are perhaps the most important contributions of our new algorithm. In addition, the program can be used to design new experiments and then test whether they would be effective in providing the data necessary to constrain important kinetic parameters.

Acknowledgments and conflict of interest

The work was supported by KinTek Corporation (Austin, TX, http://www.kintek-corp.com). We thank John Davis (University of Texas at Austin) for many helpful discussions. K.A.J. is president of KinTek, and a professional version of the software described in this article is offered for sale.

References

[1] D.M. Bates, D.G. Watts, Nonlinear Regression Analysis and Its Applications, John Wiley, New York, 1988.
[2] G.A.F. Seber, C.J. Wild, Nonlinear Regression, John Wiley, Hoboken, NJ, 2003.
[3] W.H. Press, W.T. Vetterling, B.P. Flannery, Numerical Recipes, Cambridge University Press, New York, 2007.
[4] M.A. Spies, J.J. Woodward, M.R. Watnik, M.D. Toney, Alanine racemase free energy profiles from global analyses of progress curves, J. Am. Chem. Soc. 126 (2004) 7464–7475.
[5] B.A. Barshop, R.F. Wrenn, C. Frieden, Analysis of numerical methods for computer simulation of kinetic processes: development of KINSIM––a flexible, portable system, Anal. Biochem. 130 (1983) 134–145.
[6] C.T. Zimmerle, C. Frieden, Analysis of progress curves by simulations generated by numerical integration, Biochem. J. 258 (1989) 381–387.
[7] M.R. Chernick, Bootstrap Methods: A Guide for Practitioners and Researchers, John Wiley, New York, 2007.
[8] A.C. Davison, D.V. Hinkley, Bootstrap Methods and Their Applications, Cambridge University Press, New York, 1997.
[9] B.F.J. Manly, Randomization, Bootstrap, and Monte Carlo Methods in Biology, Chapman & Hall/CRC, Boca Raton, FL, 2006.
[10] M.A. Spies, M.D. Toney, Intrinsic primary and secondary hydrogen kinetic isotope effects for alanine racemase from global analysis of progress curves, J. Am. Chem. Soc. 129 (2007) 10678–10685.
[11] K.A. Johnson, Z.B. Simpson, T. Blom, Global Kinetic Explorer: a new computer program for dynamic simulation and fitting of kinetic data, Anal. Biochem., in press, doi:10.1016/j.ab.2008.12.024.
[12] K.S. Anderson, E.W. Miles, K.A. Johnson, Serine modulates substrate channeling in tryptophan synthase: a novel intersubunit triggering mechanism, J. Biol. Chem. 266 (1991) 8020–8033.
[13] P.C. Bevilacqua, R. Kierzek, K.A. Johnson, D.H. Turner, Dynamics of ribozyme binding of substrate revealed by fluorescence-detected stopped-flow methods, Science 258 (1992) 1355–1358.